Distributed Cross-Layer Protocol Design for Magnetic Induction Communication in Wireless Underground Sensor Networks

Shih-Chun Lin, *Student Member, IEEE*, Ian F. Akyildiz, *Fellow, IEEE*,
Pu Wang, *Member, IEEE*, and Zhi Sun, *Member, IEEE*

***Abstract*—Wireless underground sensor networks (WUSNs) enable many applications such as underground pipeline monitoring, power grid maintenance, mine disaster prevention, and oil upstream monitoring among many others. While the classical electromagnetic waves do not work well in WUSNs, the magnetic induction (MI) propagation technique provides constant channel conditions via small size of antenna coils in the underground environments. In this paper, instead of adopting currently layered protocols approach, a distributed cross-layer protocol design is proposed for MI-based WUSNs. First, a detailed overview is given for different communication functionalities from physical to network layers as well as the QoS requirements of applications. Utilizing the interactions of different layer functionalities, a distributed environment-aware protocol, called DEAP, is then developed to satisfy statistical QoS guarantees and achieve both optimal energy savings and throughput gain concurrently. Simulations confirm that the proposed cross-layer protocol achieves significant energy savings, high throughput efficiency and dependable MI communication for WUSNs.**

***Index Terms*—Wireless underground sensor network, magnetic induction communication, cross-layer optimization, Pareto optimal front, distributed power control, distributed protocol.**

I. Introduction

WIRELESS underground sensor networks (WUSNs) [1] have attracted high attention for their great variety of novel applications, such as underground soil condition and power grid monitoring, mine disaster prevention and rescue, oil gas extraction, earthquake and landslide forecast, border patrol and security, and many more other applications. However, as indicated in [2], these underground environments create significant challenges for wireless communication via classical electromagnetic (EM) waves. Specifically, the main problems of EM communication rise from extremely short communication ranges, highly unreliable channel conditions, and large antenna sizes, thus making them impractical for actual deployments of WUSNs.

The magnetic induction (MI) technique [3], [4] is a promising alternative wireless communication solution to deal with the underground challenges. The MI technique utilizes the near magnetic field of coils to propagate the information, thus, achieving constant channel conditions via small size of coils. These great features make the MI communication suitable for underground environments. In [5], the channel capacity of MI communication from a pair of coil transceivers is analyzed. In [6], near-field inductive communication systems are fully investigated with regards of the channels created between two or more magnetically coupled coils. In [7], coil deployment algorithms are further proposed for MI-based WUSNs. Considering wireless power transfer, in [8], a propagation model and MI link budget are presented for wireless power transfer systems. In [9], the MI technique is further employed to efficiently transfer wireless energy over relatively long distances. Regarding the networking aspects of MI communication, in [10], the signal-to-noise ratio (SNR), connectivity, and bandwidth are examined in 3D underwater MI channels. In [11], multi-hop relay techniques are proposed to extend communication range in near-field MI communication systems. In [12], the MI-based sensors are also utilized to discriminate underground objects for military purposes. So far most of the work was done for physical layer such as antenna design, receiving signal analysis, etc. There is a lack of protocol solutions for MI-based WUSNs.

In this paper, instead of taking the classical layered protocol approach, we develop a fully distributed cross-layer protocol framework called DEAP, which fulfills a pre-defined level of quality of service (QoS). The cross-layer protocol, DEAP, considers the interactions of different layer functionalities, thus, provides efficient resource utilization and achieves high system performance. DEAP also achieves high energy savings and throughput gain with low computation complexity. First, we provide a detailed analysis on the path loss, the bandwidth, and the interference effect of the MI channel model capturing the physical layer functionalities. Furthermore, we study in detail the communication functionalities, such as modulation and forward error coding, medium access control (MAC), routing

Manuscript received January 28, 2014; revised September 13, 2014 and January 22, 2015; accepted March 8, 2015. Date of publication March 23, 2015; date of current version July 8, 2015. This research was supported by the US National Science Foundation (NSF) under Grant No. 1320758. The associate editor coordinating the review of this paper and approving it for publication was C.-B. Chae.

S.-C. Lin and I. F. Akyildiz are with the Broadband Wireless Networking Laboratory, School of Electrical and Computer Engineering, Georgia Institute of Technology, Atlanta, GA 30332 USA (e-mail: slin88@ece.gatech.edu; ian@ece.gatech.edu).

P. Wang is with the Department of Electrical Engineering and Computer Science, Wichita State University, Wichita, KS 67260 USA (e-mail: pu.wang@wichita.edu).

Z. Sun is with the Department of Electrical Engineering, State University of New York at Buffalo, Buffalo, NY 14260 USA (e-mail: zhisun@buffalo.edu).

Color versions of one or more of the figures in this paper are available online at http://ieeexplore.ieee.org.

Digital Object Identifier 10.1109/TWC.2015.2415812

algorithms, and the statistical QoS (i.e., packet delay and transmission reliability) guarantees. By integrating these functionalities we develop a cross-layer framework and provide solutions for various performance requirements of applications. Specifically, we consider the Pareto optimality for two-objective functions such as energy consumption and packet transmitted rate. The weighted sum method further converts the optimization into a single objective problem via the specific weight vectors of applications. Based on these accomplishments, we propose DEAP as the cross-layer framework in a distributed manner. In particular, we design a distributed power control via a non-cooperative game, and employ a direct sequence code division multiple access (DS-CDMA) scheme via chaotic code and utilize a geographical routing algorithm by a two-phase decision strategy. We summarize our cross-layer solution framework as follows:

1) First, we present a complete study to explore the interactions of key underground communication functionalities as well as the QoS requirements of applications.
2) A cross-layer framework is developed to integrate these functionalities for the efficient utilization of the bandwidth-limited MI communication channels.
3) DEAP is further proposed to follow the framework in a distributed manner, delivering statistical QoS guarantee and obtaining both optimal energy savings and throughput gain concurrently for practical implementation.

Simulation results show that DEAP outperforms the layered protocol solutions with 50% energy savings and 6 dB throughput gain. Moreover, beyond the centralized cross-layer designs, our solution resorts to two-phase per-node based decisions requiring only one-hop neighbor information, and has low computation complexity. Thus, by establishing reliable and efficient transmissions in challenged underground environments, we have provided a distributed cross-layer design for MI communication in WUSNs.

To the best of our knowledge, this work is the first to propose a coherent cross-layer protocol framework to optimize MI communication through a distributed approach in WUSNs. The remainder of the paper is organized as follows. The related work is given in Section II and the cross-layer communication solution is presented in Section III. Under the proposed cross-layer optimization framework, DEAP is provided to obtain optimal energy-throughput performance in Section IV. Performance evaluation is provided in Section V and the paper is concluded in Section VI.

II. Related Work

The cross-layer protocol solutions are generally recognized as a well-suitable approach for resource-efficient designs in wireless sensor networks in the last decade [13]. In the literature, many solid contributions have been extensively reported for terrestrial wireless sensor networks. In [14], the multiuser access interference (MAI) and network connectivity in wireless CDMA-based sensor networks are characterized via an integrated cross-layer study. For synchronous small-scale sensor networks, a cross-layer energy and delay optimization [15] is formulated as a convex problem to quantify the trade-off between delay and energy consumption. Furthermore, using an initiative concept, a single cross-layer module is proposed to achieve congestion control, routing, and medium access control concurrently for terrestrial wireless sensor networks [16]. A multimedia cross-layer protocol is developed for underwater acoustic sensor networks in [17] in order to support differentiated-services and to efficiently share the high-delay underwater medium. However, the challenges of wireless EM communication in underground environments [2], prevent of using the above solutions from the existing literature. In this paper, we introduce a distributed cross-layer framework for MI-based WUSNs. Our solution satisfies the QoS requirements of diverse applications, and also achieves optimal energy consumption and high throughput efficiency with low computational complexity. These features make our solution useful for practical implementations.

III. Cross-Layer Communication Solution

A. Our Cross-Layer Design

In this paper, we develop a *cross-layer resource allocation framework* that accurately models every aspect of the layered network architecture, integrates different communication functionalities into a coherent framework, and provides distributed cross-layer solutions. In order to achieve efficient MI communication in the underground environment, our solution is based on a distributed optimization problem to jointly control the *physical, MAC and routing* functionalities. In particular, our solution determines the optimal selection of modulation, FEC, and transmit power (*physical functionalities*), a DS-CDMA medium access control scheme with power control constraint to access the bandwidth-limited MI channels (*MAC functionality*), and a geographical routing algorithm (*routing functionality*). Furthermore, a cross-layer DEAP solution is proposed which is environmental-aware in capturing the underground MI channels for high utilization, and achieving low energy consumptions and limited computation complexity in WUSNs.

The remainder of this section is organized as follows. In Section III-B, we examine the MI channel model in terms of path loss, bandwidth, and interference. In Section III-C, we present possible modulation and FEC techniques suitable for the underground environment, and evaluate their performance. In Section III-D, we introduce the DS-CDMA MAC scheme and location-based routing functionalities. In Section III-E, we characterize users' application requirements of traffic QoS guarantees and provide the corresponding cross-layer constraints. Finally, in Section III-F, we discuss how to integrate and control different communication functionalities with a coherent mathematical framework. Although we present different functionalities for the sake of presentation clarity separately, the last section focuses on their coherent cross-layer integration. Note that in Table I we provide the notations used throughout the paper.

B. MI Channel Model

The MI communication link is formed by the induction between the primary and secondary coils, as an alternating

TABLE I
IMPORTANT NOTATION UTILIZED IN THIS PAPER

Notation	*Description*
r_{ij}	Distance between node i and node j
R	Resistance of coil sensor
T	Operating underground temperature
μ	Magnetic permeability of soil
σ	Electrical conductivity of soil
$L_{MI}(\cdot)$	MI path loss
$B_{MI}(\cdot)$	MI channel bandwidth
$\varepsilon_{ij}(\cdot)$	MI channel gain of link i-j
m_{ij}	Modulation technique of link i-j
$\eta(m_{ij})$	Spectrum efficiency of modulation m_{ij}
$R_{ij}(\cdot)$	Transmitted bit rate of link i-j
$\Psi_{ij}^{m_{ij}}(\cdot)$	BER of link i-j with m_{ij}
c_{ij}	FEC scheme of link i-j with rate R_C^{ij}
L	Packet length
$\Phi_{ij}(\cdot)$	PER of link i-j
Q_{ij}	Packet throughput of link i-j
Ξ_i^T	Set of interfered nodes by transmitter i
P_{ij}	Transmitted power from node i to node j
NI_j	Noise plus MAI level at node j
l_{ij}	Chaotic code length of link i-j
g_{ij}	Spreading factor of chaotic code
N_{0i}	Hop numbers from the source to node i
$N_{iD}^{(j)}$	Hop numbers from node i, via j, to the destination
S_i	Neighbor set of node i
F_i^D	Forwarding set of node i
T_{ij}	Expected packet delay of link i-j
τ	Probability bound of statistical delay guarantee
τ_{min}^j	Minimum received SINR at node j for successful transmissions
$\mathbf{w} = [w_1, w_2]^T$	Weight vector for energy savings and required throughput
$u_i(\cdot)$	Utility function of node i for power control game
$\Gamma_i(m_{ij}, T, \sigma)$	Gap between Shannon capacity and modulation m_{ij}
λ	KKT multiplier vector for optimal throughput

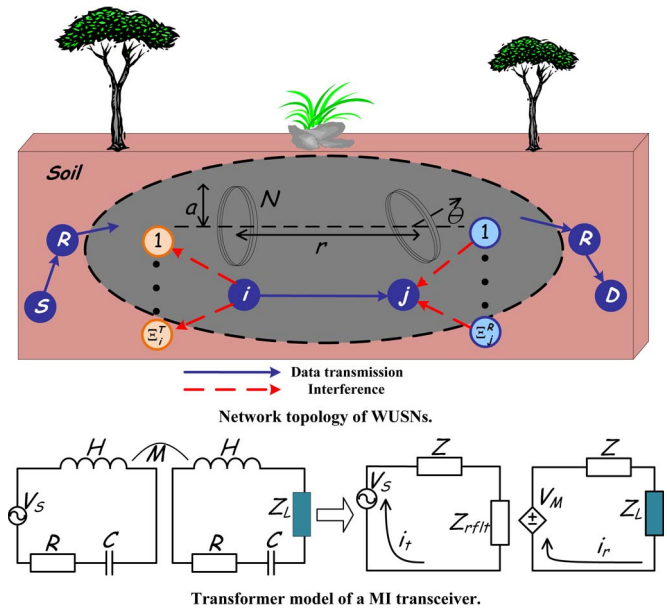

Fig. 1. Network topology of multi-hop transportation in WUSNs; a transformer model and the equivalent circuit of a transceiver coil pair $i-j$. The circuit here does not include the interference effects yet.

current exists in the primary coil. We assume that each coil has the same radius a[cm] and number of turns N. For a single transceiver in Fig. 1, r[m] is the distance between the transmitter and the receiver and θ is the angle between the axes of two coupled coils. This MI transceiver can be modeled as two transformers [18] in Fig. 1, where V_S is the voltage of transmitter's battery, Z_L is the receiver's load impedance, M is the mutual induction between two coils, R is the resistance of copper coil, H is the self induction of magnetic antenna (i.e., coil), and C is the loaded capacitor to guarantee resonance. Furthermore, the equivalent circuit of such a model is obtained as $Z = R + j\omega H + 1/(j\omega C)$, $Z_{rflt} = \omega^2 M^2/(Z + Z_L)$, and $V_M = j\omega M i_t$, where ω is the angle frequency of the transmitted signal and i_t is the current of transmitter's circuit.

As shown in [2], the magnetic permeability of the medium (i.e., soil) is the major environment factor in dominating the quality of the MI communication. Specifically, while the permeability of soil and water is similar to that of air (i.e., $\mu_0 = 4\pi \times 10^{-7}$ [H/m]) in the room temperature, such a factor and the copper resistance will change, especially for the resistance, with respect to variable temperatures in different underground depths. The medium permeability also acts differently regarding the composites of the underground magnetic contents. The entire effects are characterized as

$$\mu = \mu_0(1+\chi) = \mu_0\left(1 + p_{para}\frac{\hat{c}}{T} + p_{ferro}\chi_{ferro}\right), \quad (1)$$

$$R = 2\pi a N R_0\left[1 + \alpha_{Cu}(T - T_0)\right], \quad (2)$$

where χ and χ_{ferro} are the magnetic susceptibilities of the medium and ferromagnetic contents, p_{para} and p_{ferro} are the ratio of paramagnetic and ferromagnetic composites, $\hat{c}$ is the constant, $\alpha_{Cu} = 3.9\times10^{-3}[/^\circ\text{K}]$ is the temperature coefficient of copper coil, $T[^\circ\text{K}]$ is the actual underground temperature, and $T_0[^\circ\text{K}]$ and $R_0[\Omega/\text{m}]$ are the room temperature and the corresponding resistance of a unit length of coil. Furthermore, the self and mutual inductances, the loaded capacitance, and the receiver's impedance are also analytically obtained in the following. With the modeling of magnetic dipole for a coil, the self and mutual induction are calculated via Stoke's theorem [18]: $H \simeq \mu\pi a N^2/2$ and $M(T,\sigma) = \mu\pi N^2 a^4 G(r,\sigma)\cos\theta/4r^3$, where σ[S/m] is the medium conductivity and $G(\cdot,\cdot)$ is the attenuation factor due to the skin depth effect. Such a loss factor largely destroys the transmission quality, when encountering the salty water in the soil as explained in [19]. The capacitor is then designed to neutralize the coil impedance Z at the angle frequency of the transmitted signal, i.e., $j\omega H + 1/(j\omega C) = 0$. In addition, to maximize the transmitted power efficiency, the load impendence Z_L is designed to be the complex conjugate of the output impendence of receiver coil. Therefore, $C = 2/(\omega^2\mu\pi a N^2)$ and $Z_L = \bar{Z}$ are obtained.

Using the circuit model in Fig. 1, the path loss and the bandwidth of the MI communication are derived at the frequency of the transmitted signal (i.e., f_0 [MHz] $= \omega_0/2\pi$). The transmitted power P_t[W] of the primary coil and the received power P_r[W] of the secondary coil are $P_t = \left(Z + \frac{\omega_0^2 M^2}{Z+Z_L}\right) i_t^2 = \frac{2R^2+\omega_0^2M^2}{2R} i_t^2$ and $P_r = \left(\frac{j\omega_0 M i_t}{Z+Z_L}\right)^2 Z_L = \frac{\omega_0^2 M^2 i_t^2}{4R}$, respectively. The MI path loss L_{MI} is then obtained as

$$L_{MI}(r, f_0, \theta, T, \sigma)\ [\text{dB}] = 10\lg\frac{2\left(2R^2 + \omega_0^2 M^2\right)}{\omega_0^2 M^2} \approx 10\lg\frac{4R^2}{\omega_0^2 M^2} \triangleq 10\lg\frac{1}{\varepsilon(r, f_0, \theta, T, \sigma)}. \quad (3)$$

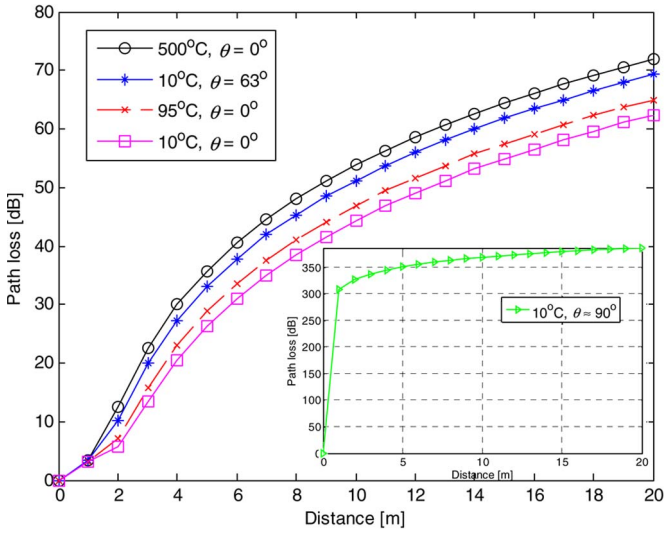

Fig. 2. Path loss of MI channels with different working temperatures and alignment angles of transceiver coils.

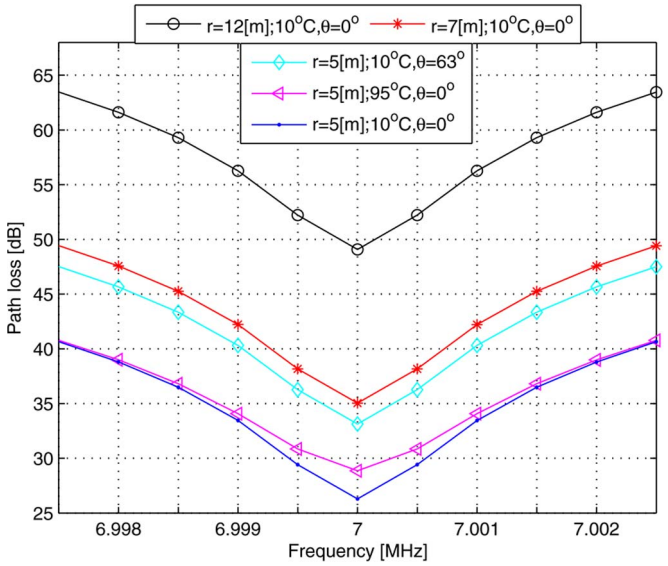

Fig. 3. Frequency response of MI channels with different transmission ranges, working temperatures, and alignment angles of transceiver coils.

While the operating frequency deviates from the central frequency f_0, the coil impendence Z is no longer pure resistance and it increases the path loss dramatically. Under this consideration, the 3-dB bandwidth $B_{MI}(T,\sigma)$[KHz] is adopted as the MI channel bandwidth. Specifically, the path loss at $f_0 + 0.5B_{MI}$ should be twice of that at f_0. Since the channel bandwidth is much smaller than the central frequency (i.e., $f_0 + 0.5B_{MI} \approx f_0$), via (3), the approximated bandwidth is thus obtained as $R(\sqrt{2}-1)/(\mu\pi^2 aN^2)$. Figs. 2 and 3 show the path losses and the frequency response of MI channels with different settings of operating scenarios. The soil composition is set as follows: the magnetic susceptibilities χ_{ferro} is $\chi_{Fe_3O_4} \approx 5\times10^{-4}$ for temperatures under 853°K as Fe_3O_4 contributes to the ferromagnetic content of most soils [20], the ratio of p_{para} and p_{ferro} are 30% and 10%, respectively, and the proportionality constant $\hat{c}$ is 0.993 (i.e., the Curie constant of iron [18]). The conductivity σ is set to 0.01 S/m for the dry soil. Other simulation parameters are set as the coil radius is 15 cm, the number of turns is 5, and the operating frequency is 7 MHz, which are favored for MI communication as suggested in [2]. In Fig. 2, as the working temperature and transmission range increase, the path loss increases accordingly and thus degrades the link transmission qualities. In addition, the impact of angle misalignment brings dramatic increasing of path loss that the transmission almost cannot take place under such cases as expected. In Fig. 3, the 3-dB bandwidth is around 1 KHz and is not affected by the transmission range and the alignment angles. On the other hand, when the working temperature increases, the bandwidth also slightly increases.

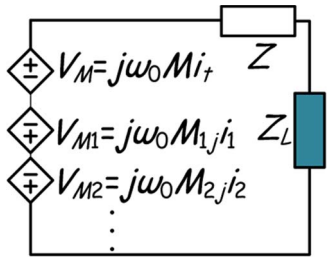

Fig. 4. Equivalent circuit for receiver coil j under the interferences.

Depicted by (3), the received power attenuates with the order of M^2 (i.e., $1/r^6$), which is much faster than the terrestrial EM communication [18] in the order of $1/r^2$. While under such high-loss circumstance, the MI transmissions between a single transceiver pair are possibly affected by adjacent communication. That is, the received signal of the receiver coil can be interfered by the neighboring transmissions with the same central frequency. Fig. 4 provides the equivalent circuit of the receiver coil j under several interferences. Assume Ξ_j^R is the set of all interfering coils of coil j as shown in Fig. 1, the received power becomes

$$\begin{aligned} P_r^j &= \left(\frac{j\omega_0\left(Mi_t - \sum_{\alpha\in\Xi_j^R} M_{\alpha j} i_\alpha\right)}{Z + Z_L}\right)^2 Z_L \\ &\approx \frac{\omega_0^2}{4R^2}\left(\sqrt{\frac{4R\varepsilon M^2 P_t}{\omega_0^2 M^2}} - \sum_{\alpha\in\Xi_j^R}\sqrt{\frac{4R\varepsilon_{\alpha j} M_{\alpha j}^2 P_\alpha}{\omega_0^2 M_{\alpha j}^2}}\right)^2 \\ &= \left(\sqrt{\varepsilon P_t} - \sum_{\alpha\in\Xi_j^R}\sqrt{\varepsilon_{\alpha j} P_\alpha}\right)^2, \end{aligned} \tag{4}$$

given $i_\alpha^2 \approx 4R\varepsilon_{\alpha j} P_\alpha/(\omega_0^2 M_{\alpha j}^2)$ from (3). Hereby we completed the analysis of the channel model for MI transceivers. Note that we conducted an experimental validation of these theoretical results through an in-lab underground testbed where the details of the testbed can be found in [21]. In addition, in the literature, there is also some discussion about the relay methods of MI waveguides that place passive coils between transceivers to amplify the received power. However, from our previous work [2], [7], the only difference between direct MI

transmission and MI waveguides is about the channel modeling. To clearly deliver our main contribution, the cross-layer design, we focus on direct MI transmission in the remainder of paper. The proposed cross-layer DEAP in Section IV is easily extensible to MI waveguides via the study in [2], [7].

C. Modulation and FEC

MI communication encounters less channel variations than the EM waves as pointed out in [2]. The undesired noise, mainly from the thermal vibration of circuit elements, lets Additive White Gaussian Noise (AWGN) to be applicable as an accurate assumption for the channel. With this in mind, the modulation and channel coding functionalities are analyzed as follows. Sophisticated modulation techniques cause more energy consumption [1] which is not desired for energy-limited WUSNs. Several simple and suitable modulation schemes, such as BPSK, BFSK, DBPSK, and 16-QAM, can be selected for WUSNs. Given the communication link $i-j$, $m_{ij} \in \mathcal{M}$ denotes the adopted modulation technique and $\eta(m_{ij})$ denotes the corresponding modulation spectrum efficiency. As bit error rate (BER) $\Psi(T,\sigma)$ usually refers to the received SNR, $\Psi_{ij}^{m_{ij}}(P_{ij}\eta B_{MI}/R_{ij}L_{MI}N_0)$ can be obtained for the modulation technique m_{ij} over link $i-j$, where N_0[W] is the thermal noise power and $R_{ij}(T,\sigma)$[bps] is the transmitted bit rate.

Regarding the channel coding schemes, the forward error correction (FEC) enhances the link transmission reliability without additional re-transmission costs and overhead, while the automatic repeat request (ARQ) does. Furthermore, the block codes have lower complexity compared to the convolutional codes (CC). In particular, a multilevel cyclic BCH (Bose, Ray-Chaudhuri, Hocquenghem) code outperforms the most energy-efficient CC by almost 15% for the optimal packet size in terrestrial wireless sensor networks as indicated in [22]. Thus, we consider the BCH code in our work. However, note that our framework can be extended to support more energy-consuming schemes, such as Reed-Solomon codes, CCs, Turbo codes as well as different types of ARQ. For the link $i-j$, $c_{ij} \in \mathcal{C}$ denotes the adopted coding scheme with coding rate R_C^{ij}. As far as $BCH(n,k,t)$ code with rate $R_C = k/n$ is concerned, n denotes the block length, k denotes the payload length, and t denotes the correcting capability of bit error (i.e., $t < n$). Given the BER $\Psi(T,\sigma)$, the block error rate Ψ_B becomes

$$\Psi_B(T,\sigma) = \sum_{i=t+1}^{n} \binom{n}{i} \Psi^i (1-\Psi)^{n-i}. \tag{5}$$

Also, with L[bit] being the packet length, the packet error rate (PER) Φ is obtained as

$$\Phi(T,\sigma) = 1 - (1-\Psi_B)^{\lceil \frac{L}{k} \rceil}, \tag{6}$$

which can be approximated as $\lceil L/k \rceil \Psi_B$ when Ψ_B is small. Fig. 5 shows PER vs. SNR for various modulation techniques and for different BCH(n,k,t) codes and no FEC scheme. The transmission range is set to 7 m and the packet length is set to 100 Bytes. Also, as suggested in the specification of soil temperature sensors in [23], the working temperature is selected as 283°K. While BPSK achieves smaller BER for any given SNR among modulation techniques, it brings the best PER performance for every channel coding schemes. In addition, while consuming more energy to perform, the powerful coding schemes (i.e., with high error correcting capability t) keep less PER for any given SNR. A trade-off exists between energy consumption and transmission quality. Our proposed cross-layer design yields an optimal trade-off point with respect to the requirements of many applications as shown later in Section III-F.

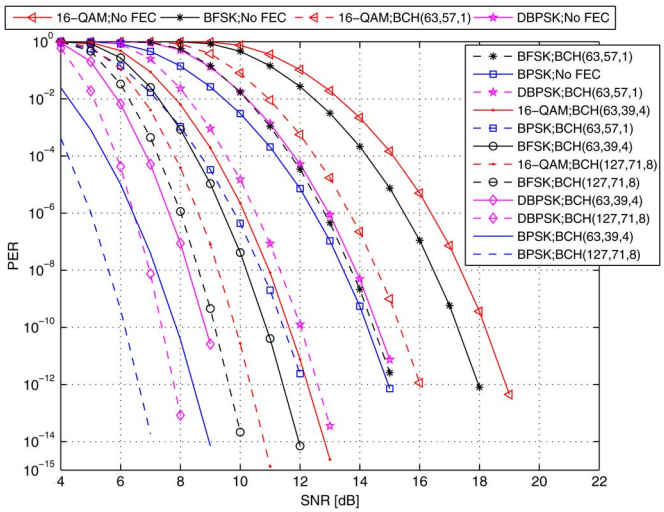

Fig. 5. Packet error rate (PER) vs. SNR for typical underground modulation techniques and BCH(n,k,t) coding schemes.

D. DS-CDMA and Geographical Routing Algorithm

Motivated by [17] in underwater acoustic sensor networks, our proposed MAC protocol, the DS-CDMA scheme compensates the drawbacks of multi-path effects and achieves high channel reuse as well as low number of packet retransmissions. Thus, it decreases the energy consumption and increases the network throughput. As chaotic codes [24] provide much higher granularity with less constraint in code properties than the pseudo-random sequences, the chaotic code with length l_{ij} [bit] $\in \mathcal{L} = [l_{min}, l_{max}]$ is adopted for transmissions over link $i-j$. The corresponding spreading factor g_{ij} is proportional to the code length (i.e., $g_{ij} = \nu l_{ij}$ with the proportional factor ν), and the transmission bit rate $R_{ij}(T,\sigma)$ becomes $\eta B_{MI}(T,\sigma)/l_{ij}$. To implement such a scheme in WUSNs, the near-far effect and MAI [25] need to be minimized. In other words, the signals arrived at the receiver should have approximately the same mean power; the interference from simultaneous transmissions of different users should also be well controlled. These are satisfied via power control design as follows.

It is assumed that r_{min}^j denotes the minimum received signal-to-interference-plus-noise ratio (SINR) of node j for successful transmissions, and the aggregated interferences to receivers are Gaussian distributed. Concerning the transmitted power level P_{ij}, the lower bound should provide r_{min}^j at node j; whereas, the upper bound should concern both the maximum power P_i^{max}[W] and the interference to nodes $k \in \Xi_i^T$, where Ξ_i^T is

the set of nodes whose ongoing communication is affected by node i's transmission as shown in Fig. 1. Specifically,

$$\begin{aligned}\varepsilon_{ij}(T,\sigma)g_{ij}P_{ij} \geq r_{min}^{j}(I_j+N_0) \Rightarrow \\ P_{ij} \geq \frac{NI_j}{g_{ij}\left(r_{min}^{j}\right)^{-1}\varepsilon_{ij}(T,\sigma)},\end{aligned} \tag{7}$$

where $\varepsilon_{ij}(T,\sigma)$ is the MI channel gain of link $i-j$ from (3) and NI_j summarizes the noise and MAI power at node j with I_j being the interference at j. Furthermore, at each node $k \in \Xi_i^T$, the following inequality should be satisfied:

$$\begin{aligned}&\left(r_{min}^{k}\right)^{-1}\varepsilon_{t_kk}(T,\sigma)g_{t_kk}P_{t_kk}-N_0-\hat{I}_k \geq \varepsilon_{ik}(T,\sigma)P_{ij} \Rightarrow \\ &\frac{\left(r_{min}^{k}\right)^{-1}g_{t_kk}P_{t_kk}\varepsilon_{t_kk}(T,\sigma)-N_0-\hat{I}_k}{\varepsilon_{ik}(T,\sigma)} = P_{ij}^{(k)}(T,\sigma) \geq P_{ij},\end{aligned} \tag{8}$$

where $\hat{I}_k$ is the interference for the transmissions of t_k to k, except the one from node i, i.e., $\hat{I}_k = (\sum_{\beta \in \Xi_k^R/\{i\}}\sqrt{\varepsilon_{\beta k}P_{\beta r_\beta}})^2$ from (4). While there are $|\Xi_i^T|$ nodes for the set Ξ_i^T, the maximum power P_{ij} with respect to these SINR requirements becomes $\min_{k\in\Xi_i^T} P_{ij}^{(k)}(T,\sigma)$. The power constraint is then

$$\frac{NI_j}{g_{ij}\left(r_{min}^{j}\right)^{-1}\varepsilon_{ij}(T,\sigma)} \leq P_{ij} \leq \min\left(\min_{k\in\Xi_i^T} P_{ij}^{(k)}(T,\sigma), P_i^{max}\right). \tag{9}$$

In our routing layer, we utilize geographical routing protocol [26], [27] because of its scalability feature and limited signaling overhead requirements. Addressing the distributed algorithm design, a source or relay node i will select its best next hop j^* with respect to the given objective function, such as E_{ij} and Q_{ij} in (15) or EaT_{ij} in (16), among the set of $S_i \cap F_i^D$. S_i is the neighbor set of node i, which includes the possible forwarder j and nodes with ongoing communication affected by i's transmissions (i.e., $S_i = \{j, \Xi_i^T\}$ followed from previous notation). F_i^D is the forwarding set, which consists of nodes closer to destination D than node i, i.e., $z \in F_i^D$ if and only if $r_{zD} < r_{iD}$. In order to expedite the per-node based decision, such geographical routing solution should map the end-to-end delay requirements into local delay requirements. Specifically, with an incoming packet to node i, the expected hop delay to node j (i.e., T_{ij}[s]) can be calculated as: $T_{ij} = \frac{T_{iD}}{N_{iD}^{(j)}} = \frac{T_{max}-(t_{now}-t_0)}{r_{iD}/(r_{iD}-r_{jD})}$, where T_{iD}[s] is the time-to-live of the arrival packet at node i, T_{max}[s] is the expected maximum end-to-end delay, t_{now} is the time when the packet arrived at node i, t_0 is the time that the packet was initially transmitted, and $N_{iD}^{(j)}$ is the expected number of hops needed from node i, via node j, to destination D. Also, the expected number of hops for the corresponding end-to-end path (i.e., from source, via link $i-j$, to destination D) is $N_{0i}+N_{iD}^{(j)}$, where N_{0i} is the number of hops that the packet traversed before it reached node i. While T_{max}, t_0, and N_{0i} can be stamped in the header of packets, r_{iD}[m] and thus $N_{iD}^{(j)}$ should be maintained via a distributed shortest-path algorithm or the underground localization mechanisms [28]. For example, as Bellman-Ford algorithm [29] is applied, $r_{iD}(t+1) = \min_{z\in S_i}(r_{iD}(t)+r_{iz})$. All the required operations and parameters are thus obtained for the proposed geographical protocol.

E. Statistical Reliability and Delay Guarantees

We study the statistical QoS in order to achieve a reliable end-to-end data transportation in WUSNs. Specifically, the higher transmission reliability associated with less packet loss is crucial for almost all types of underground sensing applications [1]. Also, the bounded delay is especially important for real-time monitoring and applications with timing constraints [30]. Aiming to support the distributed functionalities among sensors, we form the per-node based constraints (i.e., for transmissions upon link $i-j$) of link reliability and delay in the following. Given the tolerable maximum end-to-end PER Φ_T^{e2e}, the corresponding reliability constraint is

$$1-(1-\Phi_{ij}(T,\sigma))^{N_{0i}+N_{iD}^{(j)}} \leq \Phi_T^{e2e}, \tag{10}$$

where $\Phi_{ij}(T,\sigma)$ is the link PER, and $N_{0i}+N_{iD}^{(j)}$ is the expected number of traversed hops for an incoming packet to node i, which is obtained distributively as mentioned in Section III-D. Also, $\Phi_{ij}(T,\sigma)$ relates to received SINR $SINR_j(T,\sigma)$ from (5) and (6). Similarly, Φ_T^{e2e} thus provides the required r_{min}^{j} (i.e., the minimum received SINR for successful transmissions) to enable our power control functionality mentioned previously. The equivalent link constraint of (10) is then

$$SINR_j(T,\sigma) \geq r_{min}^{j}\left(\Phi_T^{e2e}\right), \tag{11}$$

where r_{min}^{j} is a function of Φ_T^{e2e}.

Furthermore, while T_{ij} provides the sample averaged link delay, the statistical delay guarantee is modeled as the probability that a packet delivered over deadline should be at most τ. That is, $\Pr(Delay \geq T_{ij}) \leq \tau$. Assume both the packet arrival time and service time upon link $i-j$ is memoryless. The service rate is $R_{ij}(T,\sigma)R_C^{ij}/L$[pkt/s] followed from previous notation and Q_{ij}[pkt/s] denotes the link (packet) throughput, which is the allowed packet arrival rate satisfying the following constraints of average link delay and delay variance in Proposition 1.

Proposition 1: For the transmission link $i-j$ with memoryless packet arrival and service time, the average delay constraints are

$$\frac{L}{R_{ij}(T,\sigma)R_C^{ij}-LQ_{ij}} \leq \tau T_{ij}, \tag{12}$$

$$LQ_{ij} < R_{ij}(T,\sigma)R_C^{ij}; \tag{13}$$

the corresponding delay variance constraint is

$$\begin{aligned}\left(\frac{L}{R_{ij}(T,\sigma)R_C^{ij}-LQ_{ij}}\right)^2 \leq \frac{\tau}{1-\tau} \\ \times\left(T_{ij}-\frac{L}{R_{ij}(T,\sigma)R_C^{ij}-LQ_{ij}}\right)^2,\end{aligned} \tag{14}$$

where τ and T_{ij} are from the QoS requirement, Q_{ij} is link throughput, L is packet length, $R_{ij}(T,\sigma)$ is transmission bit rate, and R_C^{ij} is channel coding rate.

Proof: The link delay mainly consists of the transmission delay and the queueing delay. Followed by the memoryless property, the waiting time process is exponentially distributed with mean $L/(R_{ij}R_C^{ij} - LQ_{ij})$. The Markov inequality is then applied for the QoS guarantee as $\mathbb{E}[Delay] \leq \tau T_{ij} \Rightarrow$ (12). In addition, (13) is from the stability requirement of finite link delay. Next, one-sided Chebyshev's inequality is adopted as $\Pr(Delay - \mathbb{E}[Delay] \geq T_{ij} - \mathbb{E}[Delay]) \leq \frac{\mathbb{V}[Delay]}{\mathbb{V}[Delay]+(T_{ij}-\mathbb{E}[Delay])^2}$, where $\mathbb{V}[Delay]$ denotes the delay variance and $T_{ij} - \mathbb{E}[Delay] > 0$ is satisfied by (12). By employing the condition of QoS guarantee, the following concludes the proof: $\mathbb{V}[Delay] \leq \tau\mathbb{V}[Delay] + \tau(T_{ij} - \mathbb{E}[Delay])^2 \Rightarrow$ (14). ■

F. Cross-Layer Optimization Framework

In this section, we integrate different communication functionalities mentioned above into a coherent mathematical framework and provide a unified foundation for cross-layer protocol design and control over WUSNs. The optimality of energy and throughput efficiency is reached based on application-dependent objective function. In the following, we first deal with the two-objective optimizations (i.e., with respect to the energy consumption and the system throughput), which are the two most critical factors for the energy-efficient and reliable communication. We then jointly consider the energy and throughput by using the weighted sum methods. Note that the corresponding *distributed* cross-layer solution (i.e., DEAP) is further proposed in Section IV.

1) Pareto Optimal Front and Weighted Sum Method: With the proposed distributed functionalities in WUSNs from Section III-C to Section III-E, for link $i - j$, we aim to minimize the average energy per packet for successful packet arriving at the receiver and to maximize the average transmitted packet rate, which is characterized by the allowed link throughput under the finite link delay condition (13). It is expressed as

$$\begin{aligned} &\textbf{Minimize} \quad E_{ij} = L\left(\frac{P_{ij}}{R_{ij}(T,\sigma)R_C^{ij}} + 2E_{elec}^b\right); \\ &\textbf{Maximize} \quad Q_{ij}, \end{aligned} \tag{15}$$

where $P_{ij}/(R_{ij}(T,\sigma)R_C^{ij}) + 2E_{elec}^b$ accounts for the energy to transmit one bit from node i to node j. $P_{ij}/(R_{ij}(T,\sigma)R_C^{ij})$ characterizes the distance-dependent portion of consumed energy for bit transmission, while $E_{elec}^b = E_{elec}^{trans} = E_{elec}^{rec}$[J/bit] is for the distance-independent portion. E_{elec}^{trans} and E_{elec}^{rec} come from the needed energy per bit by the transmitter and receiver electronics (e.g., VCOs, PLLs, bias currents, etc.), respectively. When confronting such multi-objective optimizations, the Pareto optimal front [31] provides the *best* solution sets that consist of non-dominated solutions, and thus provides the performance benchmarks. Fig. 6 contains these optimal points for the transmission ranges between 1 m to 15 m and the packet length 20 Bytes. While (15) belongs to *min-max* type of optimization (i.e., considering *minimizing* the energy and *maximizing* the average packet rate concurrently), the Pareto fronts should trend from lower left to upper right as verified in Fig. 6.

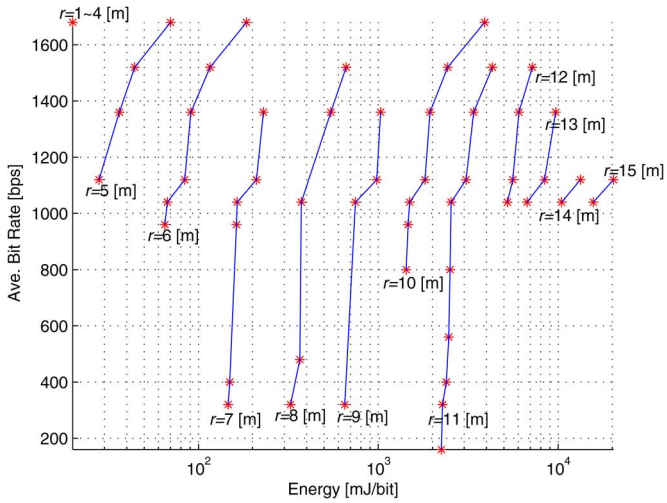

Fig. 6. Pareto optimal front for two-objective optimizations (15) with different transmission ranges.

When the transmission range increases, the minimum feasible energy consumption increases as well. Moreover, in practice, the transmission range is usually in the middle distances (i.e., between 5 m and 12 m). Fig. 6 shows that more possible Pareto points are available for such distances. Thus, more transmission parameters can be optimized under the constraints, i.e., (9), (11)–(14), for these suitable transmission ranges.

WUSN applications may have their own purposes, such as sensing the scalar data in harsh environments or monitoring the objects with high data rate requirements accompanied by possible build-in energy harvesting. These applications provide the specific weight vector $\mathbf{w} = [w_1, w_2]^T$ with $w_1 > 0$ and $w_2 > 0$ for the energy savings and required throughput. In other words, the previous two separate objective functions can be transformed into a single one (i.e., EaT for *Energy and Throughput*) via the vector and the whole optimization framework becomes

$$\begin{aligned} \textbf{Find}: \quad & T,\ \sigma,\ j \in S_i \cap F_i^D,\ m_{ij} \in \mathcal{M},\ c_{ij} \in \mathcal{C}, \\ & P_{ij} \in [0, P_i^{max}],\ Q_{ij},\ l_{ij} \in \mathcal{L} \\ \textbf{Minimize} \quad & EaT_{ij}(T,\sigma) \\ & = w_1 L\left(\frac{P_{ij}}{R_{ij}(T,\sigma)R_C^{ij}} + 2E_{elec}^b\right) - w_2 Q_{ij} \\ \textbf{Subject to} \quad & (9), (11), (12), (13), (14). \end{aligned} \tag{16}$$

The decision variables for node i are the operating temperature, the soil conductivity, the forwarder, the modulation technique, the channel coding scheme, the power level, the allowed link throughput, and the code length of DS-CDMA. Note that, to provide satisfactory cross-layer design for practical underground settings, the designated protocol needs to be environmental-aware. Specifically, it should be able to modify the corresponding transmission parameters with respect to working temperature and soil conductivity, while our environment-aware protocol yields such a capability as explained in Section IV. Furthermore, the constraint of power

control can be achieved only when a detailed link information is available to node i, which is feasible in centralized power control or under excess information broadcasting. In particular, from (9), node i needs the information about the noise plus MAI levels of its neighbors S_i (i.e., NI_j for the possible relay node j and $N_0 + \hat{I}_k$ for interfered nodes k, $\forall\, k \in \Xi_i^T$) and the user signal power levels at interfered nodes (i.e., $(r_{min}^k)^{-1} \varepsilon_{t_k k} g_{t_k k} P_{t_k k}$, $\forall\, k \in \Xi_i^T$). However, such power levels are difficult to obtain as they relate to node i's two-hop neighbors (i.e., t_k). To fix the problem and design a practical and energy-efficient power control in WUSNs, we deploy the non-cooperative game theory in Section IV-A that each sensor is able to implement a distributed power control under the limited link information.

IV. Distributed Environment-Aware Protocol (DEAP)

To empower practical applications in WUSNs, the functionalities of cross-layer framework should be distributively controlled and environmentally aware for the optimality. In the following, we first propose the distributed power control to handle the near-far effect of our DS-CDMA scheme. The structure of optimization framework is then reexamined to obtain the relationship between MAC operation and throughput performance. Finally, based on the above distributed designs, we detail the two-phase decision procedures of the proposed distributed environment-aware protocol (DEAP). In short, focusing on the functionality interactions among different layers, we are able to solve the framework in a distributed manner via its fundamental mathematical structure.

A. Distributed Power Control via Non-Cooperative Game

Instead of assuming $(NI_j; P_{ij}^{(k)}, \forall\, k \in \Xi_i^T)$ be available to node i when deciding suitable P_{ij} as (9) does, we consider the only needed information is NI_j as follows. The details for the acquirement of such information is explained in Section IV-C. A non-cooperative game $G = \{\Delta, P_i, u_i\}$ for distributed power control is formed, where there are $\Delta = 1, \ldots i, \ldots, n$ nodes transmitting on the same channel, and $P_i = [0, P_i^{max}]$ and u_i are the strategy space and the utility function of node i, respectively. Node i has the strategy $p_i \in P_i$, which provides suitable P_{ij} and we assume $P_1^{max} = \ldots = P_n^{max} = P_{max}$ for the simplicity. In a non-cooperative game, each player will select a strategy to get Nash Equilibrium (NE). In other words, a strategy that maximizes the individual utility function will be selected, i.e., $\max_{p_i \in P_i} u_i(p_i, p_{-i})$. The utility function of our power control game is defined as:

$$\begin{aligned} u_i(p_i, p_{-i}) &= \mathfrak{R}_i(p_i, p_{-i}) - \mathfrak{C}_i(p_i, p_{-i}) \\ &= w_2 B_{MI}(T, \sigma) \log_2 \left(1 + \frac{SINR_{r_i}(T, \sigma)}{\Gamma_i}\right) \\ &\quad - w_1 p_i, \end{aligned} \tag{17}$$

where $SINR_{r_i}$ denotes the SINR of node i's receiver (i.e., $SINR_j$ followed from previous notation) and Γ_i denotes the gap to the Shannon capacity that depends on the modulation scheme [32], i.e., $\Gamma_i(m_{ij}, T, \sigma) = \ln(5\Psi_{ij}^{m_{ij}}(T, \sigma))/(-1.5)$. The utility function u_i concerns a transmitted bit with respect to EaT_{ij} per packet in (16). Specifically, the revenue function $\mathfrak{R}_i$ depicts the achievable rate of link $i - j$ (i.e., $Q_{ij}L$) as a function of received SINR level [32]; the cost function $\mathfrak{C}_i$ defines the instantaneous *price* node i pays for using a specific amount of power that causes interference to other ongoing transmissions. Such cost function is linear to p_i (i.e., the transmitted power of node i). That is, rather than demanding the received SINR levels of all $k \in \Xi_i^T$ in (9), we are simply concerned with the transmitted power level p_i to quantify the impact of produced interference under the limited information.

1) Existence of the NE: The existence of the NE for the proposed power control game is provided in the following.

Definition 1: If the power strategy $P^* = (p_1^*, p_2^*, \ldots, p_n^*)$ is the NE of power control game, then for every $i \in \Delta$ and $p_i', p_i^* \in P_i$: $u_i(p_i^*, p_{-i}^*) \geq u_i(p_i', p_{-i}^*)$, where p_{-i}^* denotes the optimal strategy set of the other players.

Theorem 1: NE exists in the power control game G.

Proof: The strategy space of each node is defined as $[0, P_{max}]$, which is a nonempty, convex, and compact subset of Euclidean space $\mathbb{R}$. Also, $u_i(\cdot)$ is continuous in p_i, and from (7) and (17), we have $\frac{\partial u_i(p_i, p_{-i})}{\partial p_i} = \frac{w_2 B_{MI} \varepsilon_{ij} g_{ij}}{(NI_j \Gamma_i + \varepsilon_{ij} g_{ij} p_i) \ln 2} - w_1$ and $\frac{\partial^2 u_i(p_i, p_{-i})}{\partial p_i^2} = \frac{-w_2 B_{MI} (\varepsilon_{ij} g_{ij})^2}{(NI_j \Gamma_i + \varepsilon_{ij} g_{ij} p_i)^2 \ln 2} < 0$. Thus, $u_i(\cdot)$ is concave in p_i and the NE exists. ■

From the above proof, the global maximum is obtained when

$$p_i^* = \frac{B_{MI}(T, \sigma)}{a \ln 2} - \frac{NI_j \Gamma_i}{\varepsilon_{ij}(T, \sigma) g_{ij}}, \tag{18}$$

where $a = w_1/w_2$. Furthermore, the link reliability condition (11) is included as follows. First, from the SINR constraint in (7), $\varepsilon_{ij} g_{ij} P_{ij} / r_{min}^j - N_0 \geq I_j \Rightarrow p_i \geq NI_j r_{min}^j / (\varepsilon_{ij} g_{ij})$. Second, as the strategy p_i is in the range of $p_i = [0, P_{max}]$, the received interference of j (i.e., I_j) should be in the range of $[0, \varepsilon_{ij} g_{ij} P_{max} / r_{min}^j - N_0]$. The inequalities are then obtained as $0 \leq B_{MI}/(a \ln 2) - P_{max}\Gamma_i / r_{min}^j \leq p_i^* \leq B_{MI}/(a \ln 2) - N_0 \Gamma_i / (\varepsilon_{ij} g_{ij}) \leq P_{max}$. From (18), we have the following:

$$\begin{aligned} \frac{B_{MI} \varepsilon_{ij} g_{ij}}{(P_{max} \varepsilon_{ij} g_{ij} + N_0 \Gamma_i) \ln 2} &\leq a \\ &\leq \min\left(\frac{B_{MI} r_{min}^j}{P_{max} \Gamma_i \ln 2}, \frac{B_{MI} \varepsilon_{ij} g_{ij}}{\left(r_{min}^j + \Gamma_i\right) NI_j \ln 2}\right) \end{aligned} \tag{19}$$

Thus, the transmissions can be well established if $P_{max} \varepsilon_{ij}(T, \sigma) g_{ij} + N_0 > NI_j (r_{min}^j + \Gamma_i)$, which provides a fast inspection for reliable communication.

2) Uniqueness of the NE: To examine the uniqueness of the NE in the proposed power game, (18) should be verified as a standard function [33], which is explained in the following theorem.

Theorem 2: NE in the power control game G is unique.

Proof: See Appendix A. ■

B. The Relationship Between Code Length and Link Throughput

In this section, we aim to comprehend the relationship between the link throughput and the code lengths of DS-CDMA. Specifically, from the optimization framework in Section III-F1, the explicit form of optimal throughput Q_{ij}^* can be obtained with respect to a specific length l_{ij} by Karush-Kuhn-Tucker (KKT) conditions [31]. Considering the interested parameter Q_{ij} and the KKT multiplier vector $\lambda = [\lambda_1, \lambda_2, \lambda_3]^T$ with (16), the inequalities are obtained as follows: $\lambda \succeq 0$, $-w_2 + \lambda_1 \left(\frac{L}{R_{ij}(T,\sigma)R_C^{ij} - LQ_{ij}}\right)^2 + \lambda_2 L + 2\lambda_3 \left(\frac{L}{R_{ij}(T,\sigma)R_C^{ij} - LQ_{ij}}\right)^2 \left[\frac{L}{R_{ij}(T,\sigma)R_C^{ij} - LQ_{ij}} - \frac{\tau}{1-\tau}\left(\frac{L}{R_{ij}(T,\sigma)R_C^{ij} - LQ_{ij}} - T_{ij}\right)\right] = 0$, and $\lambda_1 \left(\frac{L}{R_{ij}(T,\sigma)R_C^{ij} - LQ_{ij}} - \tau T_{ij}\right) + \lambda_2 (LQ_{ij} - R_{ij}(T,\sigma)R_C^{ij}) + \lambda_3 \left[\left(\frac{L}{R_{ij}(T,\sigma)R_C^{ij} - LQ_{ij}}\right)^2 - \frac{\tau}{1-\tau}\left(T_{ij} - \frac{L}{R_{ij}(T,\sigma)R_C^{ij} - LQ_{ij}}\right)^2\right] = 0$. The corresponding solution is provided in Theorem 3.

Theorem 3: Given the cross-layer optimization in (16), the optimal link throughput Q_{ij}^*, regarding a specific DS-CDMA code length l_{ij} and channel coding scheme c_{ij} with rate R_C^{ij}, is

$$Q_{ij}^* = \begin{cases} \frac{R_{ij}(T,\sigma)R_C^{ij}}{L} - \frac{1}{\tau T_{ij}} & 0 \le \tau \le 0.5 \\ \frac{R_{ij}(T,\sigma)R_C^{ij}}{L} - \frac{1-A}{T_{ij}\sqrt{A}(1-\sqrt{A})} & 0.5 < \tau < 1 \end{cases}, \quad (20)$$

where A equals to $\tau/(1-\tau)$.

Proof: See Appendix B. ■

While the code length of DS-CDMA (and thus the transmission bit rate $R_{ij}(T,\sigma) = \eta B_{MI}(T,\sigma)/l_{ij}$) has been shown in connection with the power level and the link throughput, respectively, an one-dimensional-search approach can be applied to decide the optimal l_{ij}^* corresponded to the minimum link metric in (16). Specifically, via (18) and (20), the link metric EaT_{ij} becomes the function of the code length only regarding a specific neighbor j of node i, a modulation technique m_{ij}, and a channel coding scheme c_{ij} with rate R_C^{ij}. Then, the golden section approach [31] can be applied to provide a sufficient accuracy for the minimizer. That is, given $l_{ij} \in \mathcal{L} = [l_{min}, l_{max}]$, the uncertainty range for l_{ij}^* after K_l steps of reduction turns into $(1-\rho)^K(l_{max} - l_{min})$, where $1 - \rho = 0.618$.

C. Algorithm: Two-Phase Decision Strategy

Utilizing the distributed designs of cross-layer functionalities in Section IV-A and Section IV-B, we propose the distributed two-phase operation that follows the cross-layer framework in (16) as follows. Inherited from the per-node based geographical routing paradigm in Section III-D, the sender i (i.e., source or relay node) optimally decouples the cross-layer optimization (and thus routing decision) into two sub-problems and solves them sequentially as:

1) Minimize the link metric EaT_{ij} with respect to the power level P_{ij}, the allowed link throughput Q_{ij}, and the code length of DS-CDMA l_{ij} for each of its feasible next-hop neighbors and possible combinations of modulation and channel coding functionalities, i.e., $(j; m_{ij}; c_{ij})$.
2) Select the best next-hop j^* and the physical functionalities $(m_{ij}^*; c_{ij}^*)$ associated with the best link metric.

Rather than solving a complicated optimization problem for the best route to destination, a generic node i only needs to sequentially deal with two low-complexity sub-problems without loss of optimality. Algorithm 1 presents a space-search approach to solve the first sub-problem, whose complexity is $O(|\mathcal{M}| \cdot |\mathcal{C}| \cdot K_l)$, where $|\mathcal{M}|$, $|\mathcal{C}|$, and K_l are the number of modulation techniques, FEC schemes, and reduction steps for optimal chaotic code length, respectively. It makes use of the Algorithm 2 to obtain three communication parameters (i.e., P_{ij}, Q_{ij}, and l_{ij}), via distributed power control, KKT optimality, and golden section search [31]. The second sub-problem can be expressed as $j^* = arg\min_{j \in S_i \cap F_i^D} EaT_{ij}$, guiding the route geographically to the destination (i.e., by selecting $j \in S_i \cap F_i^D$). It has a complexity $O(|S_i \cap F_i^D|)$, proportional to the number of the sender's neighboring nodes within its forwarding set towards the destination. Note that, in order to capture the underground environment, sender i first measures the operating temperature T and conductivity σ of the surrounding soil. The measurements of these crucial factors can be carried out by the sensing units of current off-the-shelf sensors [23], [34], [35]. Sender i then employs these measurements to facilitate the proposed environment-aware cross-layer framework, i.e., (16). Furthermore, the only required link information for solving these two sub-problems is the interference levels of sender i's certain neighbors (i.e., $NI_j, \forall\, j \in S_i \cap F_i^D$) from the distributed power control design. Instead of applying inefficient broadcasting for such information, a short message is exchanged by using a common chaotic code l_C known by all devices. In particular, sender i transmits a short request to nodes in $S_i \cap F_i^D$ for their interference levels. The information is then sent back via l_C by those who successfully receive node i's request. In summary, the above operations do not need to be performed every time a sensor has a packet to route, but execute only when the physical channel or traffic conditions have changed. As a sender does not have the global knowledge of the network, our cross-layer link approach does not guarantee the global optimality, but achieves the best feasible performance given the limited information at the sender. Furthermore, with the distributed power control design, the stacks of functionalities from physical to network layers can work fully distributively, especially crucial for practical applications in WUSNs from their resource-limited nature of signaling message exchanges.

Algorithm 1 Distributed Cross-layer Link Optimization

Input: i, j, r_{ij}, θ_{ij}
1: $EaT_{min} = \infty$ % Initialization
2: **for** $mod = 1 : |\mathcal{M}|$ **do** % Modulation cycle
3: **for** $fec = 1 : |\mathcal{C}|$ **do** % FEC cycle
4: **Calculate** r_{min}^j via tolerable end-to-end PER Φ_T^{e2e}
5: $(EaT_{ij}, P, Q, l) \leftarrow$**Algorithm 2**$(r_{min}^j, NI_j, r_{ij}, \theta_{ij},$
6: $m_{ij}(mod), c_{ij}(fec))$
7: **if** $EaT_{ij} < EaT_{min}$ **then**
8: $EaT_{min} = EaT_{ij}$
9: $(m, c, P, Q, l)^* = (m(mod), c(fec), P, Q, l)$

Algorithm 2 Link Parameters

Input: $r^j_{min}, NI_j, r, \theta, m, c$
Output: EaT^*, P^*, Q^*, l^*
1: **Get** $EaT(l)$ in (16) via (18), (20), $(r^j_{min}, NI_j, r, \theta, m, c)$
2: $l^* \leftarrow$**GoldenSection**$(EaT(l), K_l)$ % K_l:Reduction steps
3: **Calculate** P^*, Q^*, EaT^* by l^*, (16), (18), and (20)

Once the optimization problem is solved at sender i, the optimal communication parameters are attained by node i (i.e., j^*, m_{ij^*}, c_{ij^*}, P_{ij^*}, l_{ij^*}, and Q_{ij^*}) for data payload transmissions. In order to enable such transmission, certain procedures for control signaling are still needed and explained as follows. Instead of sending control packets with additional resource consumption, the extended header (EH) is sent using l_C via a random access scheme (such as ALOHA-like or CSMA-like MAC [29]). Specifically, sender i transmits a short header EH followed by its actual data packet (i.e., payload plus standard header) to the chosen next-hop j^*. Such an EH contains information about l_{ij^*} that sender i will use for the subsequent data packets and the information of other parameters (i.e., m_{ij^*} and c_{ij^*}). If no collision happens for the EH transmission (i.e., i is the only node transmitting an EH in the neighborhood of node j^*), j^* will synchronize to the signal from node i, despread the EH using l_C, and set its decoder according to the optimal parameters used by i for the subsequent data packet decoding. Once node j^* has correctly received the packet from i, it sends an acknowledge (ACK) packet back with code l_A. If sender i does not receive ACK before a timeout expires, it follows the procedures of chosen random access schemes to recover from collisions. The whole signaling operations are summarized in Fig. 7. These simple but efficient procedures indeed facilitate the DEAP design.

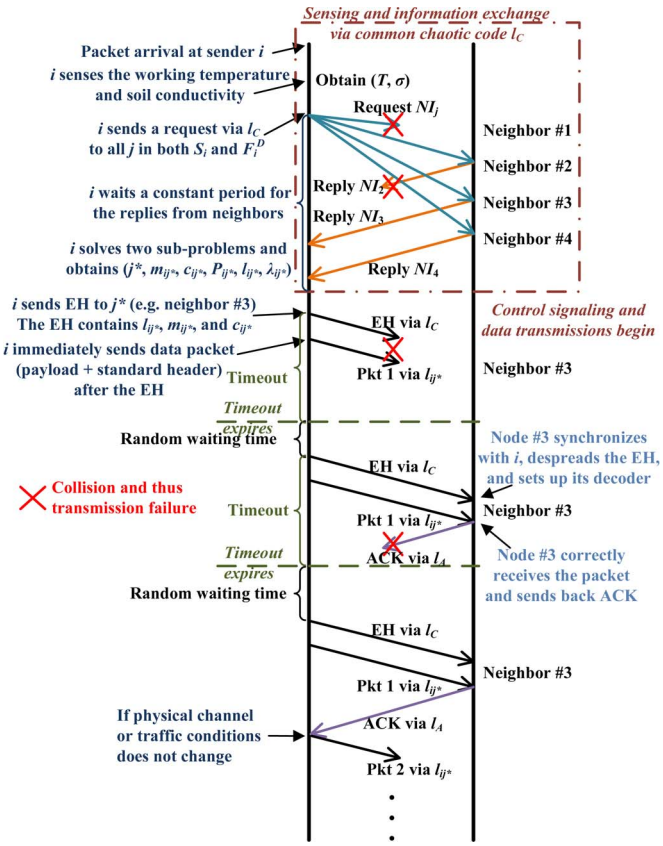

Fig. 7. Timing diagram of DEAP with ALOHA-like [29] random access scheme.

V. Performance Evaluation

We compare the performance of the proposed DEAP in Section IV with the traditional layered protocol solutions (i.e., individual communication functionalities do not share information and operate in separate layers). Simulation results confirm that DEAP achieves remarkable energy savings as well as high throughput gain in a distributed manner, favored by practical implementation in WUSNs. In the following, we first evaluate the performance of link transmissions and then examine the end-to-end communication.

A. Link Transmissions

Considering the interactions among physical layer functionalities (i.e., modulation techniques, channel coding schemes, and power control design), the energy consumption per bit, transmit power, and average bit rate are evaluated with respect to different MI transmission ranges. The comparison for DEAP is carried out with two fixed modulation/FEC combinations selected from Section III-C, i.e., BPSK/No FEC and BFSK/BCH(63,57,1), and one cross-layer design following the framework in Section III-F that provides centralized power control by (9) in Section III-D. The QoS requirements for the transmissions are set as follows: the expected hop delay 0.9 s, the outage delay probability should be less than 0.8, and the maximal tolerable PER is 10^{-4} with packet length 20 Byte. Also, the weight vector from application is set as $w_1 = 0.7$ for energy consumption and $w_2 = 0.3$ for link throughput, and the high interference scenario is concerned with 0.02 W noise plus MAI power level.

In Figs. 8 and 9, the transmitted energy and power of fixed modulation/FEC combinations for a successfully decoded payload bit at the receiver are always higher than the cross-layer designs. Furthermore, regarding the cross-layer solutions, as centralized power control assumes more available network information (i.e., both one-hop and two-hop neighbors' transmitted power level as explained in Section III-F1), it gives lower energy consumption and power level than the proposed distributed solution (i.e., DEAP). However, such assumption can only be achieved theoretically via a great deal of control signaling exchanges, which is impossible in the practical energy-limited scenarios such as WUSNs. On the other hand, DEAP permits the only needed information of transmitter to become the received noise plus MAI power level at the receiver (i.e., one-hop neighbors' info). It provides the energy consumption close to the centralized one and even achieves the same level under long transmission distances. The impact of coil angle misalignment is also presented for the cross-layer design, while the layered schemes cannot obtain the solution with practical

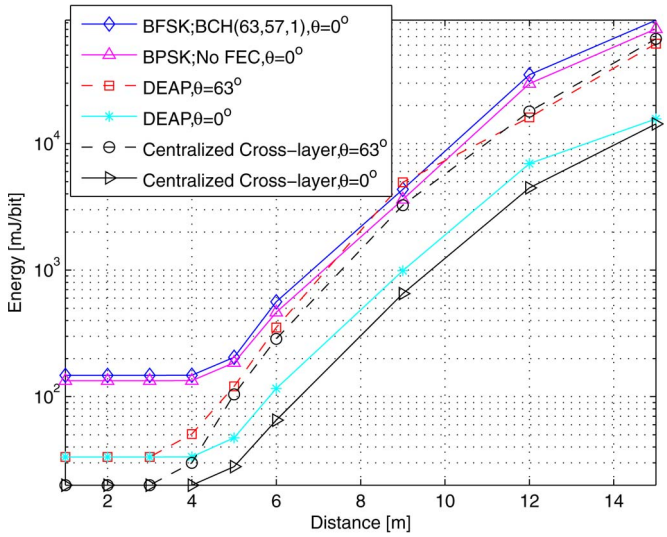

Fig. 8. Energy per bit for the centralized cross-layer solution, the cross-layer DEAP, and two fixed modulation/FEC combinations.

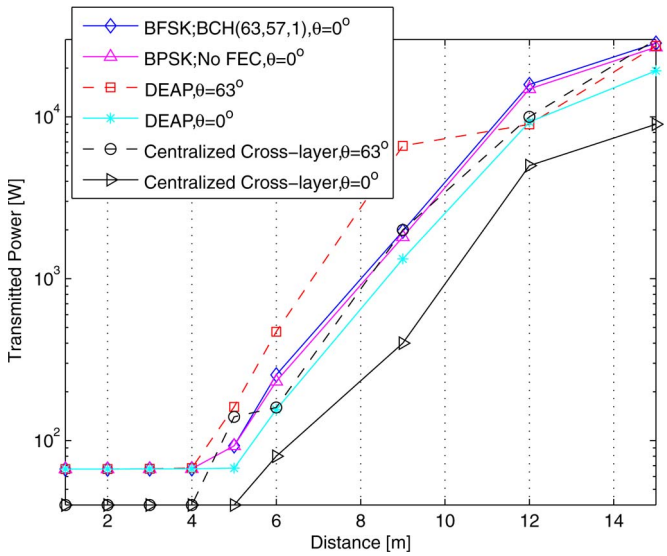

Fig. 9. Transmitted power for the centralized cross-layer solution, the cross-layer DEAP, and two fixed modulation/FEC combinations.

applications. Under this setting, the consumed energy of DEAP and the centralized designs are almost the same even under short transmission distances.

Fig. 10 further provides the achievable average bit rates with respect to layered solutions (i.e., BFSK; BCH (63, 57, 1) and BPSK; No FEC) and cross-layer solutions (i.e., Centralized Cross-layer and DEAP). Cross-layer design is favored for its higher bit rate as compared to the layered solution. Also, the proposed DEAP outperforms the centralized scheme for nearly all transmission distances and allows much higher bit rate, especially under middle transmission ranges. The reason is that our distributed solution does not confined by the severe power constraints from two-hop neighbors as centralized solution does, which always considers the worst-case scenario. Instead, DEAP employs a non-cooperative game to distributively control each sensor's transmitted power, thus enjoying higher throughput.

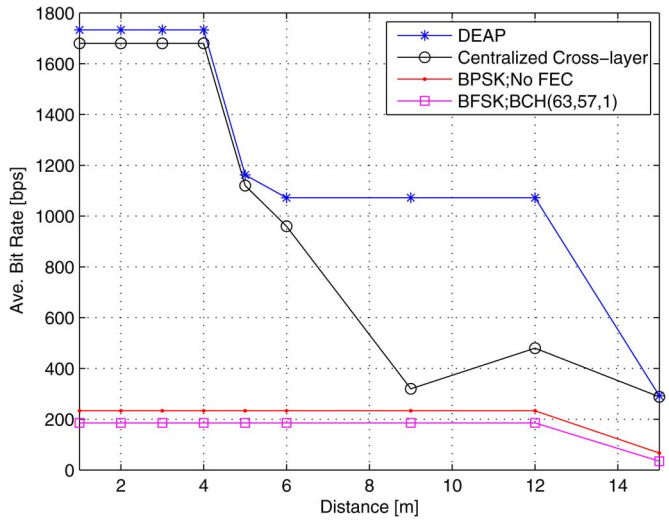

Fig. 10. Average bit rate for the centralized cross-layer solution, the cross-layer DEAP, and two fixed modulation/FEC combinations.

To sum up, DEAP not only achieves almost the same level of energy consumption as the centralized design, but brings remarkable link throughput over bandwidth-limited MI communication channels. It also provides much lower computation complexity as discussed previously in Section IV-C for great practicability in WUSNs.

B. End-to-End Data Flow

The interactions between MAC and routing functionalities are examined via end-to-end energy and throughput performance. Two layered protocol architectures (i.e., GEO and TPL) are built for the comparison with our proposed design. The detail configurations are explained as follows:

[GEO] Geographical Routing (Section III-D) + DS-CDMA (Section III-D and IV-B) + Distributed Power Control (Section IV-A) + MI Channel Model (Section III-B): This protocol configuration employs previously proposed distributed power control and DS-CDMA (via chaotic code) scheme for physical and MAC layer, respectively. For the routing algorithm, it reduces the distance from the transmitter to the destination by selecting the next closet node to the destination as the next hop.

[TPL] TPL-Based Greedy Routing + DS-CDMA (Section III-D and IV-B) + Distributed Power Control (Section IV-A) + MI Channel Model (Section III-B): This protocol configuration is much similar to GEO, except that the routing decision is based on the channel quality of the transmitter with its neighbors. The channel quality is measured in terms of the transmitted power level (TPL) for successfully bit decoding at the receiver. The node that minimizes the required transmitted power the most is selected as the next hop.

While the above layered GEO and TPL apply previously proposed functionalities more or less, they only consider their related layers without information sharing but with reasonable assumptions for the other layers. These architectures along with our distributed design are evaluated in a 3D underground cube with the volume $10 \times 10 \times 10$ m^3. A variable number

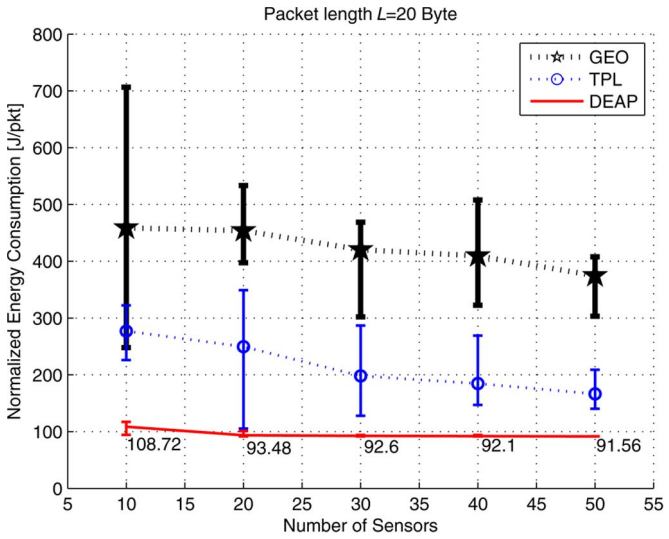

Fig. 11. Normalized energy consumption for the cross-layer DEAP and the layered protocols of TPL and GEO.

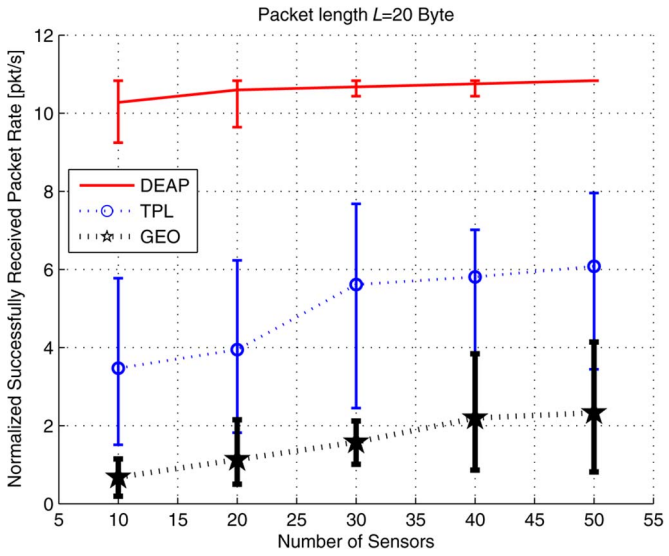

Fig. 12. Normalized successfully received packet rate for the cross-layer DEAP and the layered protocols of TPL and GEO.

of sensors (from 10 to 50) are uniformly deployed in such an area, as three source-destination pairs are randomly selected among them. Also, to approach more practical and reasonable scenarios, the maximum transmission range of a transceiver pair is restricted to 12 m suggested by the previous results in Section V-A, as it costs too much energy and gets little throughput under too long distance.

Figs. 11 and 12 show the normalized energy and successfully received packet rate for end-to-end data flow. As the number of sensor increases, there exists more *good routes* (i.e., those provide better end-to-end performance) and the greater cooperative diversity is thus obtained. Such advantages are revealed by less energy consumption and more achievable throughput in all three protocols. Specifically, without exchanging the information among different layer functionalities and adopting layered approach, GEO selects the set of nodes that sequentially move closest to the destination, mainly concerning the geographical progression and providing the worst performance. As for TPL, it minimizes the required transmitted power along the multi-hop transportation, which trades more link transmissions (and thus longer routes) for better energy savings. Aiming at yielding the best energy and throughput performance concurrently, our schemes surpass both GEO and TPL protocols with at least 50% energy savings and 6 dB throughput gain. It comes from the fact that jointly optimizing the communication functionalities of different layers brings great *synergies* to improve end-to-end system performance. These outstanding energy and spectral efficiencies accompanied with low computational complexity confirm that the proposed DEAP well suits underground environments. Therefore, we introduce a new paradigm for reliable and efficient MI communication and offer a novel avenue towards distributed cross-layer design in WUSNs.

VI. Conclusion

In this paper, the interaction of key underground communication functionalities is addressed and a distributed cross-layer design, the distributed environment-aware protocol (DEAP), is developed to efficiently utilize the bandwidth-limited MI channels in WUSNs. Leveraging a non-cooperative game, a designated distributed power control enables the DS-CDMA mechanism via chaotic codes for reliable link transmissions under limited available network information. Furthermore, by analytically solving the cross-layer framework with respect to the given code length, statistical delay constraints are guaranteed and the optimal link throughput is achieved. Upon these accomplishments, a two-phase decision strategy is employed to sequentially tackle two sub-problems for the best feasible energy savings and throughput gain, enjoying low computation complexity for great practicability. Performance evaluation confirms that the DEAP provides high system throughput and very low energy consumption within a guaranteed delay.

Appendix A
The Uniqueness of NE

Let $p=(p_i,p_{-i})$ and $f(p)=B_{MI}/(a\ln 2)-NI_j\Gamma_i/(\varepsilon_{ij}g_{ij})$. We prove that $f(p)$ is a standard function, as it preserves the positivity, monotonicity, and the extendibility.

- Positivity: the condition of $f(p)>0$ is equivalent as $B_{MI}\varepsilon_{ij}g_{ij}/(NI_j\Gamma_i\ln 2)>a$. It is satisfied via (19). If $B_{MI}r^j_{min}/(P_{max}\Gamma_i\ln 2)\geq B_{MI}\varepsilon_{ij}g_{ij}/[(r^j_{min}+\Gamma_i)NI_j\ln 2]$, $a\leq\frac{B_{MI}\varepsilon_{ij}g_{ij}}{(r^j_{min}+\Gamma_i)NI_j\ln 2}<\frac{B_{MI}\varepsilon_{ij}g_{ij}}{\Gamma_iNI_j\ln 2}$; otherwise, $a\leq\frac{B_{MI}r^j_{min}}{P_{max}\Gamma_i\ln 2}=\frac{B_{MI}\varepsilon_{ij}g_{ij}}{(\max\{I_j\}+N_0)\Gamma_i\ln 2}<\frac{B_{MI}\varepsilon_{ij}g_{ij}}{\Gamma_iNI_j\ln 2}$. Thus, $f(p)$ is positive.
- Monotonicity: from (4), I_j is analytically derived as $\sum_{\alpha=1,\alpha\neq i}^{n}h_{\alpha j}P_{\alpha r_\alpha}=(\sum_{\alpha=1,\alpha\neq i}^{n}\sqrt{\varepsilon_{\alpha j}p_\alpha})^2$. If $p_i\geq p_i$ for every $i\in\Delta$, $f(p')-f(p)=\frac{I_j(p)-I_j(p')}{\varepsilon_{ij}g_{ij}}=\frac{\left(\left[\sum_{\alpha=1,\alpha\neq i}^{n}\sqrt{\varepsilon_{\alpha j}p_\alpha}\right]^2-\left[\sum_{\alpha=1,\alpha\neq i}^{n}\sqrt{\varepsilon_{\alpha j}p_\alpha}\right]^2\right)\Gamma_i}{\varepsilon_{ij}g_{ij}}\leq 0$, which means $f(p)$ is monotonously decreasing.

- Extendibility: for every $c > 1$, we have $cf(p) - f(cp) = (c-1)[B_{MI}/(a \ln 2) - N_0\Gamma_i/(\varepsilon_{ij} g_{ij})]$. According to the statement for the positivity, $a < \frac{B_{MI}\varepsilon_{ij}g_{ij}}{\Gamma_i N I_j \ln 2} < \frac{B_{MI}\varepsilon_{ij}g_{ij}}{N_0\Gamma_i \ln 2}$, which implies $cf(p) - f(cp) > 0$ and $f(p)$ is extendible.

Thus, $f(p)$ is a standard function with an unique fixed point; the NE is unique in this game.

APPENDIX B
THE OPTIMAL LINK THROUGHPUT

To ease the derivation, set A equal to $\tau/(1-\tau)$ and y equal to $L/(R_{ij}R_C^{ij} - LQ_{ij})$. Then, the inequalities in Section IV-B are simplified as $\lambda_1 \geq 0$, $\lambda_2 \geq 0$, $\lambda_3 \geq 0$, $-w_2 + \lambda_1 y^2 + \lambda_2 L + 2\lambda_3 y^2[y - A(y - T_{ij})] = 0$, and $\lambda_1(y - \tau T_{ij}) + \lambda_2(-Ly^{-1}) + \lambda_3[y^2 - A(T_{ij} - y)^2] = 0$. Considering the possible values for KKT multipliers, we have $\lambda_2 = 0$, as $LQ_{ij} - R_{ij}R_C^{ij} < 0$ due to finite link delay. Also, for λ_1 and λ_3: 1) $\lambda_1 = 0$, $\lambda_3 = 0$: no possible solution since w_2 is assumed to be positive; 2) $\lambda_1 > 0$, $\lambda_3 = 0$: when $A < 1$, $y = \tau T_{ij}$, $\lambda_1 = w_2/(\tau^2 T_{ij}^2)$, and $Q_{ij}^{(1)} = R_{ij}R_C^{ij}/L - 1/(\tau T_{ij})$; 3) $\lambda_1 = 0$, $\lambda_3 > 0$: when $A > 1$, $y^2 = A(T_{ij} - y)^2$, $\lambda_3 = w_2(1-A)^2/[2(T_{ij}\sqrt{A})^3(1-\sqrt{A})^2]$, and $Q_{ij}^{(2)} = R_{ij}R_C^{ij}/L - (1-A)/[T_{ij}\sqrt{A}(1-\sqrt{A})]$; 4) $\lambda_1 > 0$, $\lambda_3 > 0$: when $A = 1$, $y = T_{ij}/2$, $\lambda_1 + 2T_{ij}\lambda_3 = 4w_2/T_{ij}^2$, and $Q_{ij}^{(3)} = R_{ij}R_C^{ij}/L - 2/T_{ij}$. The second-order test [31] is then easy to take. Thus, in summary, for $A \leq 1$, $Q_{ij}^* = Q_{ij}^{(1)}$; for $A > 1$, $Q_{ij}^* = Q_{ij}^{(2)}$.

REFERENCES

[1] I. F. Akyildiz and E. P. Stuntebeck, "Wireless underground sensor networks: Research challenges," *Ad Hoc Netw.*, vol. 4, no. 6, pp. 669–686, Nov. 2006.

[2] Z. Sun and I. F. Akyildiz, "Magnetic induction communications for wireless underground sensor networks," *IEEE Trans. Antennas Propag.*, vol. 58, no. 7, pp. 2426–2435, Jul. 2010.

[3] J. J. Sojdehei, P. N. Wrathall, and D. F. Dinn, "Magneto-Inductive (MI) communications," in *Proc. MTS/IEEE Conf. Exhib.*, Nov. 2001, vol. 1, pp. 513–519.

[4] R. Bansal, "Near-field magnetic communication," *IEEE Antennas Propag. Mag.*, vol. 46, no. 2, pp. 114–115, Apr. 2004.

[5] S. Kisseleff, I. F. Akyildiz, and W. Gerstacker, "Throughput of the magnetic induction based wireless underground sensor networks: Key optimization techniques," *IEEE Trans. Commun.*, vol. 62, no. 12, pp. 4426–4439, Dec. 2014.

[6] J. I. Agbinya, "Investigation of near field inductive communication system models, channels and experiments," *Progr. Electromagn. Res. B*, vol. 49, pp. 129–153, 2013.

[7] Z. Sun and I. F. Akyildiz, "Optimal deployment for magnetic induction-based wireless networks in challenged environments," *IEEE Trans. Wireless Commun.*, vol. 12, no. 3, pp. 996–1005, Mar. 2013.

[8] J. I. Agbinya, "A magneto-inductive link budget for wireless power transfer and inductive communication systems," *Progr. Electromagn. Res. C*, vol. 37, pp. 15–28, 2013.

[9] A. Karalis, J. D. Joannopoulos, and M. Soljacic, "Efficient wireless non-radiative mid-range energy transfer," *Ann. Phys.*, vol. 323, no. 1, pp. 34–48, Jan. 2008.

[10] B. Gulbahar and O. B. Akan, "A communication theoretical modeling and analysis of underwater magneto-inductive wireless channels," *IEEE Trans. Wireless Commun.*, vol. 11, no. 9, pp. 3326–3334, Sep. 2012.

[11] M. Masihpour, D. Franklin, and M. Abolhasan, "Multihop relay techniques for communication range extension in near-field magnetic induction communication systems," *J. Netw.*, vol. 8, no. 5, pp. 999–1011, May 2013.

[12] T. H. Bell, B. J. Barrow, and J. T. Miller, "Subsurface discrimination using electromagnetic induction sensors," *IEEE Trans. Geosci. Remote Sens.*, vol. 39, no. 6, pp. 1286–1293, Jun. 2001.

[13] X. Lin, N. B. Shroff, and R. Srikant, "A tutorial on cross-layer optimization in wireless networks," *IEEE J. Sel. Areas Commun.*, vol. 24, no. 8, pp. 1452–1463, Aug. 2006.

[14] S. De, C. Qiao, D. A. Pados, M. Chatterjee, and S. J. Philip, "An integrated cross-layer study of wireless CDMA sensor networks," *IEEE J. Sel. Areas Commun.*, vol. 22, no. 7, pp. 1271–1285, Sep. 2004.

[15] S. Cui, R. Madan, A. J. Goldsmith, and S. Lall, "Cross-layer energy and delay optimization in small-scale sensor networks," *IEEE Trans. Wireless Commun.*, vol. 6, no. 10, pp. 3688–3699, Oct. 2007.

[16] M. C. Vuran and I. F. Akyildiz, "XLP: A cross-layer protocol for efficient communication in wireless sensor networks," *IEEE Trans. Mobile Comput.*, vol. 9, no. 11, pp. 1578–1591, Nov. 2010.

[17] D. Pompili and I. F. Akyildiz, "A multimedia cross-layer protocol for underwater acoustic sensor networks," *IEEE Trans. Wireless Commun.*, vol. 9, no. 9, pp. 2924–2933, Sep. 2010.

[18] D. R. Frank, *Electromagnetic Theory*. Englewood Cliffs, NJ, USA: Prentice-Hall, 1986.

[19] S. Kisseleff, W. Gerstacker, R. Schober, Z. Sun, and I. F. Akyildiz, "Channel capacity of magnetic induction based wireless underground sensor networks under practical constraints," in *Proc. IEEE WCNC*, Apr. 2013, pp. 2603–2608.

[20] C. E. Mullins, "Magnetic susceptibility of the soil and its significance in soil science: A review," *J. Soil Sci.*, vol. 28, no. 2, pp. 223–246, Jun. 1977.

[21] X. Tan, Z. Sun, and I. F. Akyildiz, "A testbed of magnetic induction-based communication system for underground applications," *IEEE Antennas Propag. Mag.*, [Online]. Available: http://arxiv.org/abs/1503.02519

[22] Y. Sankarasubramaniam, I. F. Akyildiz, and S. W. McLaughlin, "Energy efficiency based packet size optimization in wireless sensor networks," in *Proc. IEEE SNPA*, Apr. 2003, pp. 1–8.

[23] Campbell Scientific, Logan, UT, USA, Soil temperature sensors. [Online]. Available: http://www.campbellsci.com

[24] G. Mazzini, G. Setti, and R. Rovatti, "Chaotic complex spreading sequences for asynchronous DS-CDMA. i. system modeling and results," *IEEE Trans. Circuits Syst. I, Fundam. Theory Appl.*, vol. 44, no. 10, pp. 937–947, Oct. 1997.

[25] C. S. Chang and K. C. Chen, "Medium access protocol design for delay-guaranteed multicode CDMA multimedia networks," *IEEE Trans. Wireless Commun.*, vol. 2, no. 6, pp. 1159–1167, Nov. 2003.

[26] D. Pompili, T. Melodia, and I. F. Akyildiz, "Routing algorithms for delay-insensitive and delay-sensitive applications in underwater sensor networks," in *Proc. ACM Conf. MobiCom Netw.*, 2006, pp. 298–309.

[27] H. Zhang and H. Shen, "Energy-efficient beaconless geographic routing in wireless sensor networks," *IEEE Trans. Parallel Distrib. Syst.*, vol. 21, no. 6, pp. 881–896, Jun. 2010.

[28] A. Magnani and K. K. Leung, "Self-organized, scalable GPS-free localization of wireless sensors," in *Proc. IEEE WCNC*, Mar. 2007, pp. 3798–3803.

[29] D. Bertsekas and R. Gallager, *Data Networks*. Englewood Cliffs, NJ, USA: Prentice-Hall, 1987.

[30] M. D. Bedford and G. A. Kennedy, "Evaluation of zigbee (IEEE 802.15.4) time-of-flight-based distance measurement for application in emergency underground navigation," *IEEE Trans. Antennas Propag.*, vol. 60, no. 5, pp. 2502–2510, May 2012.

[31] E. K. P. Chong and S. H. Zak, *An Introduction to Optimization*, 3rd ed. Hoboken, NJ, USA: Wiley, 2008.

[32] J. R. Barry, E. A. Lee, and D. G. Messerschmitt, *Digital Communication*. 3rd ed. Boston, MA, USA: Kluwer, 2004.

[33] R. D. Yates, "A framework for uplink power control in cellular radio systems," *IEEE J. Sel. Areas Commun.*, vol. 13, no. 7, pp. 1341–1347, Sep. 1995.

[34] Decagon Devices, Pullman, WA, USA, 5TE Soil Moisture, Temperature, and Electrical Conductivity. [Online]. Available: http://www.decagon.com/products/soils/volumetric-water-content-sensors/5te-vwc-ec-temp/

[35] Delta-T Devices, Cambridge, U.K., WET-2 Sensor (Water Content, EC, and Temperature). [Online]. Available: http://www.delta-t.co.uk/product-display.asp?id=WET-2 Product-div=Soil Science

Shih-Chun Lin (S'08) received the B.S. degree in electrical engineering and the M.S. degree in communication engineering from National Taiwan University in 2008 and 2010, respectively. Currently, he is working toward the Ph.D. degree in electrical and computer engineering under the supervision of Prof. Ian F. Akyildiz. He is a Graduate Research Assistant in the Broadband Wireless Networking (BWN) Laboratory, School of Electrical and Computer Engineering, Georgia Institute of Technology. His research interests include wireless underground sensor networks, software defined networking, large machine-to-machine communication, cognitive radio networks, and statistical scheduling in wireless systems.

Ian F. Akyildiz (M'86–SM'89–F'96) received the B.S., M.S., and Ph.D. degrees in computer engineering from the University of Erlangen-Nurnberg, Germany, in 1978, 1981 and 1984, respectively. Currently, he is the Ken Byers Chair Professor in Telecommunications with the School of Electrical and Computer Engineering, Georgia Institute of Technology (Georgia Tech), Atlanta, GA USA; the Director of the Broadband Wireless Networking (BWN) Laboratory and the Chair of the Telecommunication Group at Georgia Tech. Since 2013, he is a Finland Distinguished Professor Program (FiDiPro) Professor (supported by the Academy of Science) with the Department of Electronics and Communications Engineering, Tampere University of Technology, Finland, and the Founding Director of the Nano Communications Center (NCC). Since 2008, he is also an Honorary Professor with the School of Electrical Engineering, Universitat Politcnica de Catalunya (UPC), Barcelona, Catalunya, Spain, and the Founding Director of the NaNoNetworking Center in Catalunya (N3Cat). Since 2011, he is a Consulting Chair Professor at the Department of Information Technology, King Abdulaziz University (KAU), Jeddah, Saudi Arabia. He is the Editor-in-Chief of *Computer Networks (Elsevier) Journal*, and the founding Editor-in-Chief of the *Ad Hoc Networks (Elsevier) Journal*, the *Physical Communication (Elsevier) Journal* and the *Nano Communication Networks (Elsevier) Journal*. He is an IEEE Fellow (1996) and an ACM Fellow (1997). He received numerous awards from IEEE and ACM. His h-index is 88 and the total number of citations is above 69K due to Google scholar as of March 2015. His current research interests are in wireless sensor networks in challenged environments, 5G cellular systems, nanonetworks, terahertz band, and software defined networks.

Pu Wang (M'05) received the B.S. degree in electrical engineering from the Beijing Institute of Technology, Beijing, China, in 2003, the M.Eng. degree in computer engineering from the Memorial University of Newfoundland, St. Johns, NL, Canada, in 2008, and the Ph.D. degree in electrical and computer engineering from the Georgia Institute of Technology, Atlanta, GA, USA, in 2013. He is currently an Assistant Professor with the Department of Electrical Engineering and Computer Science, Wichita State University, Wichita, KS, USA. He received the BWN Lab Researcher of the Year Award in 2012, from Georgia Institute of Technology. He received the TPC Top Ranked Paper Award of IEEE DySPAN 2011. He was also named a Fellow of the School of Graduate Studies, 2008, Memorial University of Newfoundland. His research interests include wireless sensor networks, cognitive radio networks, software defined networks, nanonetworks, multimedia communications, wireless communications in challenged environment, and cyber-physical systems.

Zhi Sun (M'11) received the B.S. degree in telecommunication engineering from Beijing University of Posts and Telecommunications (BUPT), and the M.S. degree in electronic engineering from Tsinghua University, Beijing, China, in 2004 and 2007, respectively, and the Ph.D. degree in electrical and computer engineering from Georgia Institute of Technology, Atlanta, GA, USA, in 2011, under the guidance of Prof. Dr. Ian F. Akyildiz. Currently, he is Assistant Professor in the Electrical Engineering Department, State University of New York at Buffalo, Buffalo, NY, USA. Prior to that, he was a Postdoctoral Fellow at Georgia Institute of Technology. He won the Best Paper Award in the 2010 IEEE Global Communications Conference (Globecom). He received the BWN Researcher of the Year Award at Georgia Institute of Technology in 2009. He was also given the Outstanding Graduate Award at Tsinghua University in 2007. His expertise and research interests lie in wireless communications, wireless sensor networks, and cyber physical systems in challenged environments.